NUMERICAL EXPLORATION OF ELECTRONIC, DYNAMIC AND OPTICAL PROPERTIES OF InI-AgBr HETEROSTRUCTURE FOR OPTOELECTRONIC APPLICATION

[1]Popoola, A. I., [2]Adetunji B. I., [1]Odusote, Y. A. and [1]Adewale, J. O.

DOI 10.51459/jostir.2025.1.2.0144

[1]*Department of Physics, Federal University of Technology Akure, Ondo State, Nigeria*

[2]*Physical Sciences Department, Bells University of Technology, Ota, Ogun State, Nigeria*

ABSTRACT

Innovation in technology has been influenced by optoelectronic devices and their applications, with silicon playing a major role. Advanced functionalities, including high density data storage, efficient energy harvesting etc has necessitated the search for novel materials. Heterostructure formation is a newer method for developing semiconductor of better functionality. The calculation of the electronic structure, optical properties, and dynamic stability of a non-silicon material (InI-AgBr heterostructure) are reported. Like silicon, the aim is to evaluate the prospect of InI-AgBr heterostructure for photovoltaic energy harvesting. The results predict InI-AgBr single-layer heterostructure to be an indirect bandgap semiconductor (Eg ≈ 1.120 eV) with an effective interlayer distance of 0.4046 nm. The optoelectronic indices, including extinction coefficient and the electron energy loss are excellent compared to that of silicon. The calculated refractive index is 4.75, much above the threshold value of 1, while the absorption coefficient is good and predicted to increase with additional heterostructure layers. Overall, InI-AgBr single-layer heterostructure is predicted to be a valuable semiconductor for optoelectronic device fabrication.

Keywords: *bandgap, optoelectronics, extinction index, heterostructure*

Correspondence
aipopoola@futa.edu.ng/ispopoola71@gmail.com

History
Received: 02/04/2025
Accepted: 20/07/2025
Published: 10/11/2025

https://www.futa.edu.ng

JOSTIR
JOURNAL OF SCIENCE, TECHNOLOGY AND INNOVATION RESEARCH
https://jostir.futa.edu.ng

1 | Introduction

There are presently quests to maximally utilize renewable energy resources and the two area of application in which improved optoelectronic devices are mostly sought are photovoltaic and photocatalysis. For photovoltaic applications, silicon (Si) still remained the most widely used material, accounting for ~ 80% of the market despite an abysmally low efficiency (~ 26 %). For higher photovoltaic efficiency, a number of semiconductors including, Gallium Arsenide (GaAs), organic Perovskites, nanocrystalline films and active quantum dots (Yamaguchi, 2021; García de Arquer *et al*., 2021; Adeyinka *et al*., 2023; Machin and Márquez, 2024; Grim *et al*., 2015; Noman *et al*., 2024) have showed promise. While efficiencies higher than 30 % have been reported, Gallium (Ga) for example is unfortunately more expensive than Si and Arsenic (As) is poisonous. Additionally, fabricating optoelectronic devices using these alternative means have been found to be expensive. Finding an alternative to Si that are not toxic, abundant, and relatively inexpensive is a challenge that require enormous technological undertakings.

Any post 26 % and 30 % efficient photovoltaic material, is expected to see enhancements regarding high photon absorption, high carrier generation/mobility and high carrier separation and collection at the electrodes (Merupo *et al.*,2023; Lin *et al.*, 2021). With the fascinating material properties (i.e. structural, electronic, and optical) observed in $MoSSe/WSe_2$ and graphene/PbI_2 heterostructures, two-Dimensional (2D) materials and heterostructures have become a veritable way to provide unique properties engineering that can help resolve single material shortcomings such as low quantum efficiency, high charge recombination, and band-structure anomalies (Liu *et al.*, 2015; Khan *et al.*, 2020; Lin *et al.*, 2023; Yuan et al., 2017; Phogat *et al.*, 2024; Shen *et al.*, 2024). Aside optoelectronic applications, 2D heterostructures that possess magnetic character, such as $CrBr_3/NbSe_2$, CoFeB/MgO etc are unravelling compelling opportunities in spintronics, with emerging devices such as the magnetic tunneling junctions (MTJ) devices, spin field-effect transistors, and memristors relevant to quantum computing (Bingyu *et al.*, 2024). According to Ki *et al* (2025), 2D nanomaterials are increasingly becoming relevant for biosensing applications on the account of their unique intrinsic physicochemical properties. To develop high-performance biosensors that can be integrated into advanced biomedical systems is relatively easy because 2D structures, including graphene, transition metal dichalcogenides (TMDCs), and MXenes can be easily customized at the atomic and molecular levels leading to the enhanced sensitivity, selectivity, mechanical flexibility, and biocompatibility of the sensors (Wang *et al.*, 2022; Liu *et al.*, 2023; Sakthivel *et al.*, 2023).

Scientists have in recent times intensified efforts to apply the numerical methods such as the Density Functional Theory (DFT) to critically investigate and design new semiconductor materials especially from among 2D materials and heterostructures due to the tendency for layer thicknesses impact on materials properties in 2D materials and heterostructures (Liang et al., 2018; Xuan *et al.*,2023; Cai *et al.*,2023). A heterostructure is investigated and discussed in this article. It has been formed between indium iodide (InI) and silver bromide (AgBr). The dynamic stability as well as the electronic structure and optical properties are investigated to evaluate the suitability of the heterostructure to fabricate optoelectronic devices.

2. | Computational Details

Monolayers of InI and AgBr were created and stacked to form InI/AgBr heterostructure using the VESTA software (Momma and Izumi, 2011). Thereafter, the structures geometry was optimized to obtain a relaxed compound. This was followed by calculating the optimum interlayer distance between the heterostructure monolayers. The electronic band structure, dynamic stability as well as the optoelectronic parameters, such as the absorption coefficient, refractive index, extinction coefficient etc were evaluated. All calculations were done using the Quantum Espresso Package (Giannozzi *et al.*, 2009; Giannozzi *et al.*, 2017; Giannozzi *et al.*, 2020). In all cases, the Generalized Gradient Approximated functional developed by Perdew-Burke-Ernzerhof (PBE) was used for the geometry optimizations and bandstructure calculations (Perdew *et al.*, 1996).
Both the ultrasoft (US) and norm-conserving (NC) pseudopotentials with full relativistic (FR) effects were used (Vanderbilt, 1990). Being 2D material, the k mesh sampling was 12 × 12 × 1 at wave function expansion energy cut-off of 900eV. The total energy and forces convergence criteria were set to 10^{-8} eV and 0.001 eV A^{-1} respectively. The lattice dynamic stability was evaluated using the

Density Functional Perturbation Theory (Baroni *et al.*, 2001)

The aforementioned parameters were used to carry out a Self-Consistent Field (SCF) and band calculations. The binding energy E_b was obtained from the ground state energies as:

$$E_b = E_{(InI|AgBr)} - E_{InI} - E_{AgBr} \quad (1)$$

where $E_{(InI|AgBr)}$ is the ground state energy of the heterostructure formed, E_{InI} is the energy of InI monolayer, and E_{AgBr} is the energy of AgBr monolayer. The dielectric function that relates to the optical properties is given as:

$$\boldsymbol{\varepsilon} = \boldsymbol{\varepsilon}_1(\omega) + i\varepsilon_2(\omega) \quad (2)$$

where ε_2 is the imaginary part and ε_1 is the real part and both are functions of the incident photon frequency (ω). Using the dielectric functions terms (ε_2 and ε_1), we can derived the following optical properties expressions:

$$\alpha(\omega) = \frac{\omega}{c}\sqrt{2\left(\sqrt{\varepsilon_1^2(\omega) + \varepsilon_2^2(\omega)} - \varepsilon_1(\omega)\right)} \quad (3)$$

$$n(\omega) = \sqrt{\left(\frac{\varepsilon_1(\omega) + \sqrt{\varepsilon_1^2(\omega) + \varepsilon_2^2(\omega)}}{2}\right)} \quad (4)$$

$$k(\omega) = \sqrt{\frac{-\varepsilon_1(\omega) + \sqrt{\varepsilon_1^2(\omega) + \varepsilon_2^2(\omega)}}{2}} \quad (5)$$

$$L(\omega) = \frac{\varepsilon_2(\omega)}{\varepsilon_2(\omega)^2 + \varepsilon_1(\omega)^2} \quad (6)$$

where α(ω) is the absorption index, L(ω) is the electron loss function, n(ω) is the refractive index and k(ω) is the extinction index.

3. | Results and Discussion

3.1 | Structural and Electronic properties

InI and AgBr are 2D materials with the P$\bar{3}$m1 Strubericht notation (space group number 91). Their bulk phase structures are shown in Figure 1 (a) & (c), while the monolayers created with the VESTA program are shown in Figures 1 (b) and (d) respectively. There are four different options for stacking monolayer of InI on AgBr to form InI-AgBr heterostructure. These stacking options are shown in Figure 2 (a) – (d). In Fig. 2(a), Iodide (I) and Bromine (Br) were the nearest neighbors across the Interlayer Distance (I_D). Indium (In) and Br were the nearest neighbors in Figure 2(b). It is silver (Ag) and I in 2(c) while it is Ag and In in Figure 2(d) respectively.

The most stable stacking was determined by evaluating the ground state energy of each of the phases in Figure 2 and the result is given in Table 1. According to Table 1, phase III is the most stable phase and the optimized interlayer distance for this phase is given in Figure 3. The determined sufficient value is 0.4046 nm.

When a material is formed, different bonds are shared by the elements. This determine the type of materials formed. In DFT, material types (metals, semiconductors and insulators) can be evaluated through band structure calculations. The accuracy of bandstructure results, depends on the type of functional used, the quality of the calculation, and how well the calculated structure is represented. The bandstructure result of InI-AgBr heterostructure alongside InI and AgBr bulk phases are given in Figure 4. It can be seen that InI is an indirect bandgap semiconductor while AgBr is a direct bandgap semiconductor. This agrees with available literature data (Gjerding *et al.*, 2021).

The bandgaps, measured by calculating the difference between the Valence Band Maximum (VBM) and the Conduction Band Minimum (CBM) showed that AgBr (Eg = 1.770 eV) is a

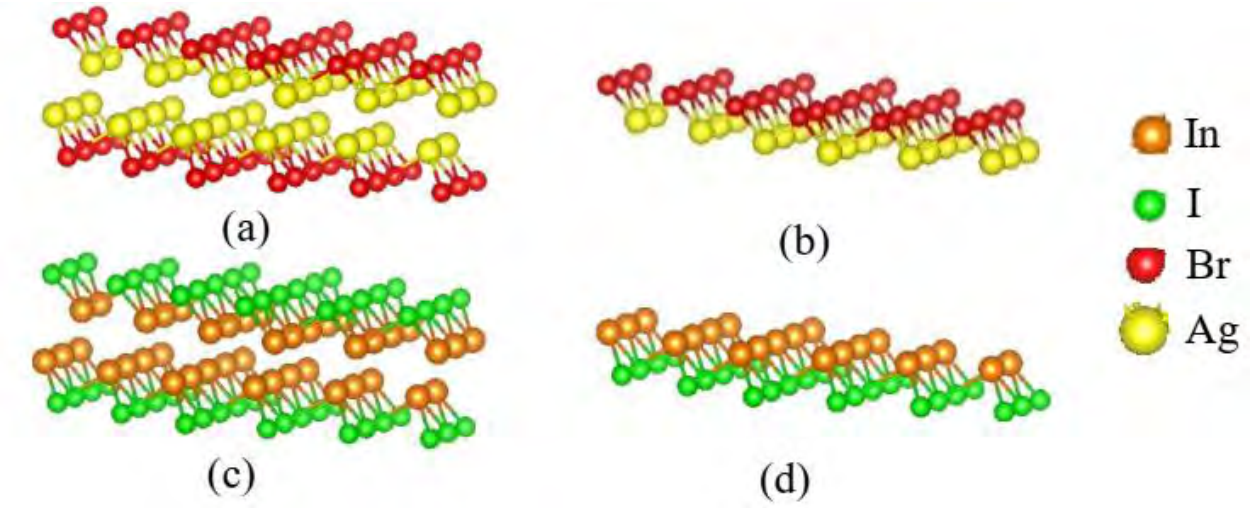

Figure 1 | (a) The Crystal structure of hexagonal Silver Bromide (AgBr), (b) AgBr monolayer, (c) crystal structure of hexagonal Indium Iodide (InI) and (d) InI monolayer.

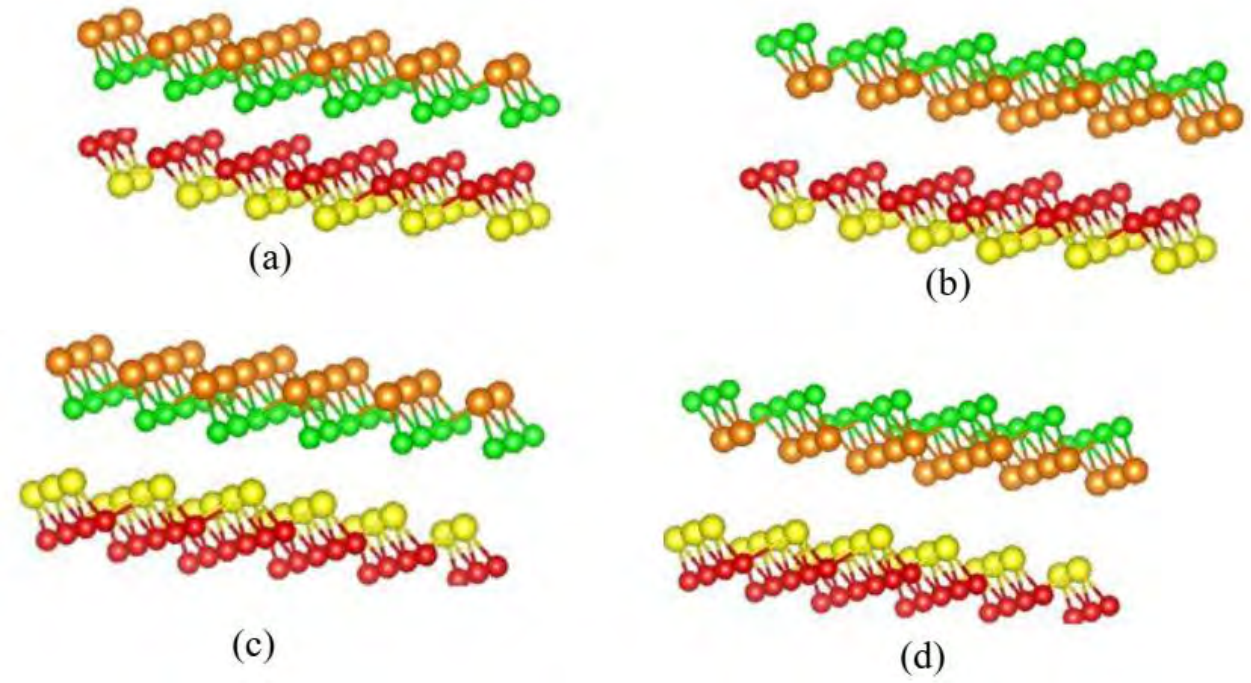

Figure 2 | (a) Heterostructure of InI/AgBr Phase I, (b) heterostructure of InI/AgBr Phase II, (c) heterostructure of InI/AgBr Phase III, (d) heterostructure of InI/AgBr Phase IV.
Images in Figures 1 and 2 created with VESTA.

wider bandgap material compared to InI (*E*g = 1.036 eV). The difference in *E*g results and available literature values (*E*g = 0.988 eV for InI and 1.724 eV for AgBr), gives a difference of only 4.8 % (InI) and 4.6 % (AgBr) respectively. With the consistency exhibited by the results, it can be concluded that the results are reliable. The bandgap results from more precise but highly sophisticated hybrid functional (HSE) had predicted *E*g = 1.335 eV for InI and 2.962 eV for AgBr respectively. Since GGA usually under-estimates bandgap (in the range between 40 – 50 %), it can be agreed that

Table 1 | Calculated ground state energy of InI-AgBr Phases

Phase	Energy (Ry)
I	-509.311
II	-509.302
III	-509.327
IV	-509.307

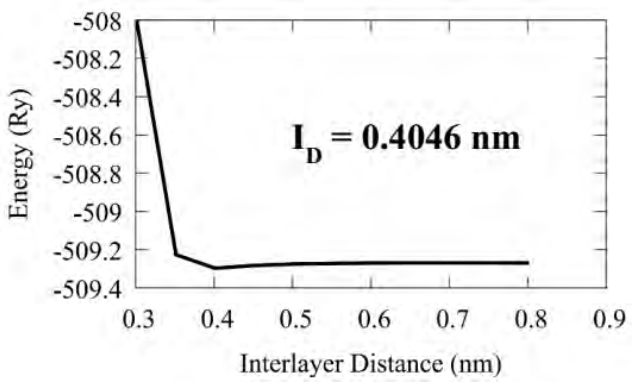

Figure 3 | Calculated Interlayer Distance (I_D) for the most stable phase of InI-AgBr heterostructure.

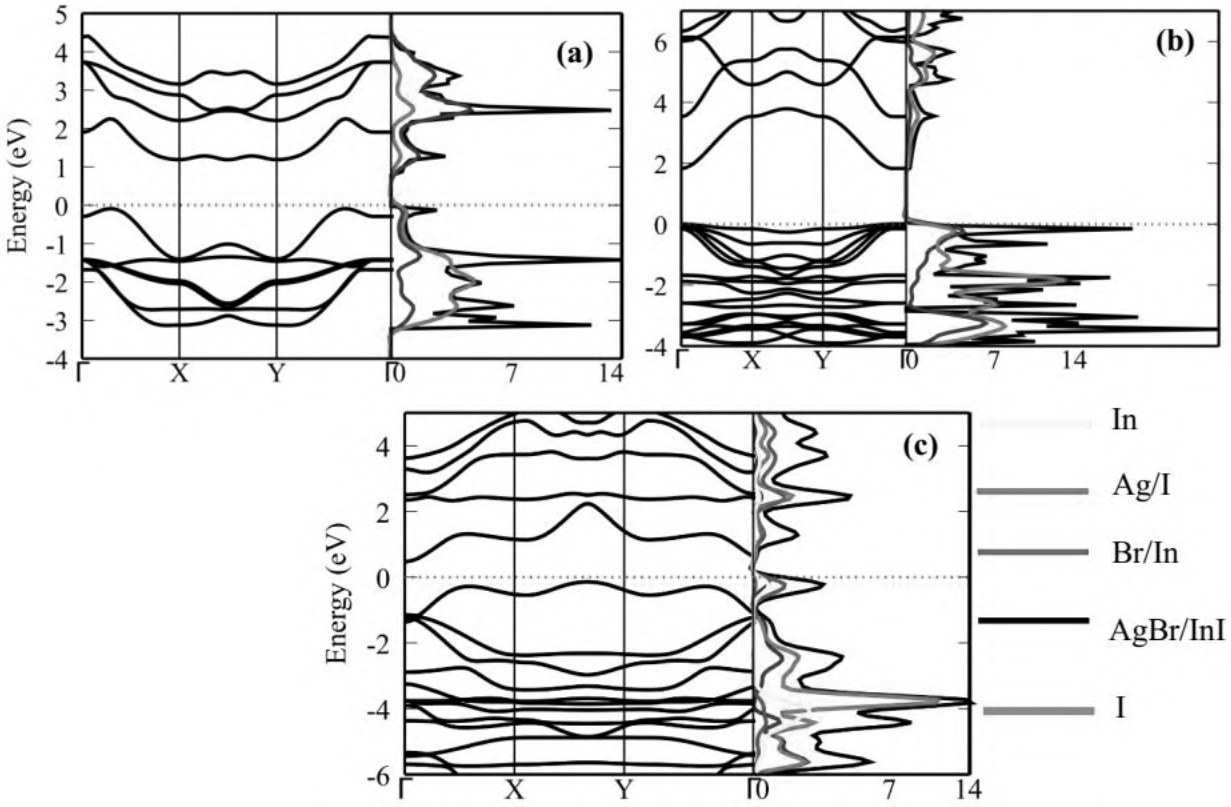

Figure 4 | Calculated bandstructure of (a) InI, (b) AgBr and (c) InI-AgBr heterostructure. The Fermi level is marked by the dotted red lines and have been shifted to zero energy level.

the bandgap of InI is of order ~ 1.335 eV and that of AgBr ~ 2.962 eV.

Based on the confidence in the results of Figure 4 (a) & (b), the bandstructure of InI-AgBr was calculated and given in Figure 4 (c). It can be predicted that a single layer of InI-AgBr heterostructure is an indirect bandgap semiconductor with GGA-PBE derived E_g = 0.864 eV. This value could approach ~ 1.296 eV (if the 50 % underestimation margin is considered), making it to almost be equivalent to the 1.120 eV for silicon.

The Density of States (DoS) which has been plotted alongside the bandstructure in Figure. 4 gives a similar result except for its inability to identify the material type. It can help identify constituent/element contributions to material formation. In InI for example (Figure 4 (a)), Indium is the dominating element contributing to InI formation within the conduction band. It is Br at the conduction band and Ag at the valence band for AgBr. In the case of the InI-AgBr heterostructure, there is a segmentation of energy bands within which the contribution of each element is relevant. From the edge of the bandgap through the conduction band (~ 0.2 – 5 eV), strong hybridization occurred between In and Ag. From the Fermi level down the valence band (~0 to -2 eV), the hybridization of Ag and Br can be observed. It can thus be concluded that the contribution of Iodide to InI-AgBr heterostructure formation is weak.

3.2 | Phonon dispersion

Phonons are crucial to the understanding of thermal and mechanical properties of materials. While photons are carriers of electromagnetic force, fundamental to optics and electromagnetism, phonons are carriers of vibrational energy in solids. In photovoltaic devices, phonons can cause properties enhancement such as increased electron generation, improved light absorption and better transport of charge carriers, all of which are capable of efficiency improvements in solar cells. The computed phonon dispersion of InI, AgBr and InI/AgBr heterostructre along the high symmetric Brillouin zone path Γ-X-Y-Γ is illustrated in Figure 5. The splitting between Transverse and Longitudinal Optical (TO-LO) modes along Brillouin zone path indicates, as expected that long range coulomb interactions are active in all the three semiconductors. The acoustic phonons are obtained in the energy range of 0 – 5.43 meV for InI, 0 – 5.21 meV for AgBr, 0 meV for InI/AgBr. The optical phonons are obtained in the energy range of 2.4 – 17.5 meV for InI, 2.89 – 17.30 meV for AgBr and 1.85 – 29.26 meV for the InI/AgBr heterostructure. With higher energy optical phonons obtained in InI/AgBr heterostructure than InI and AgBr alone, better light absorption is predicted through phonon activities. Additionally, all the semiconductor compounds (InI, AgBr and InI/AgBr heterostructure) are dynamically stable

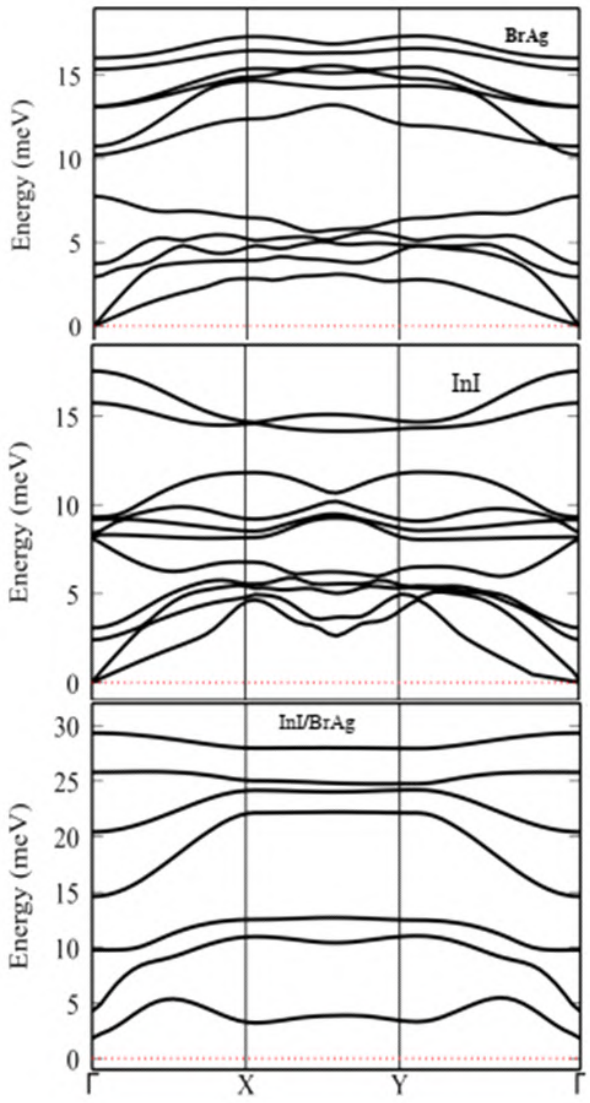

Figure 5 | Calculated phonon dispersion for InI, AgBr and the InI-AgBr heterostructure. No dispersion is observed below the dotted red lines, showing no phonon with negative frequencies.

as none of the compounds had negative frequency/energy in its dispersion.

3.3 | Optical properties

The calculated result for the optical indices is given in Figure 6. Light absorbers, as in the case of photovoltaic cells should demonstrate high light absorption coefficient within the *E*g. Compared with InI and AgBr compounds, the heterostructure showed better absorption coefficient. Materials with refractive index above 1 are regarded good

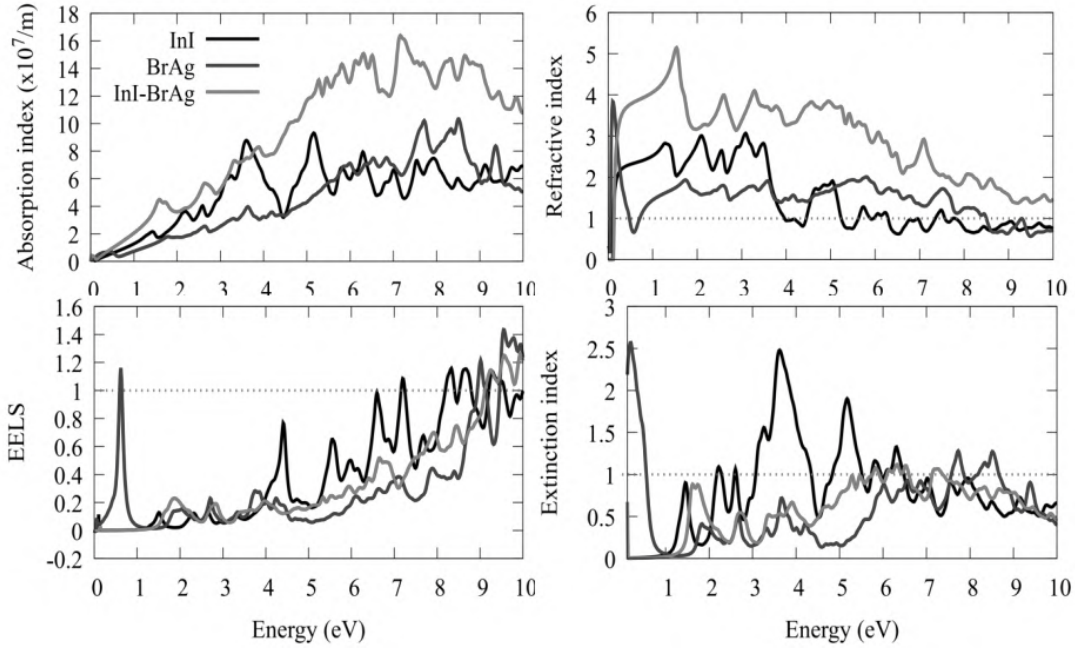

Figure 6 | Calculated refractive index, absorption coefficient, extinction index and the EELS for InI, AgBr and InI-AgBr heterostructure.

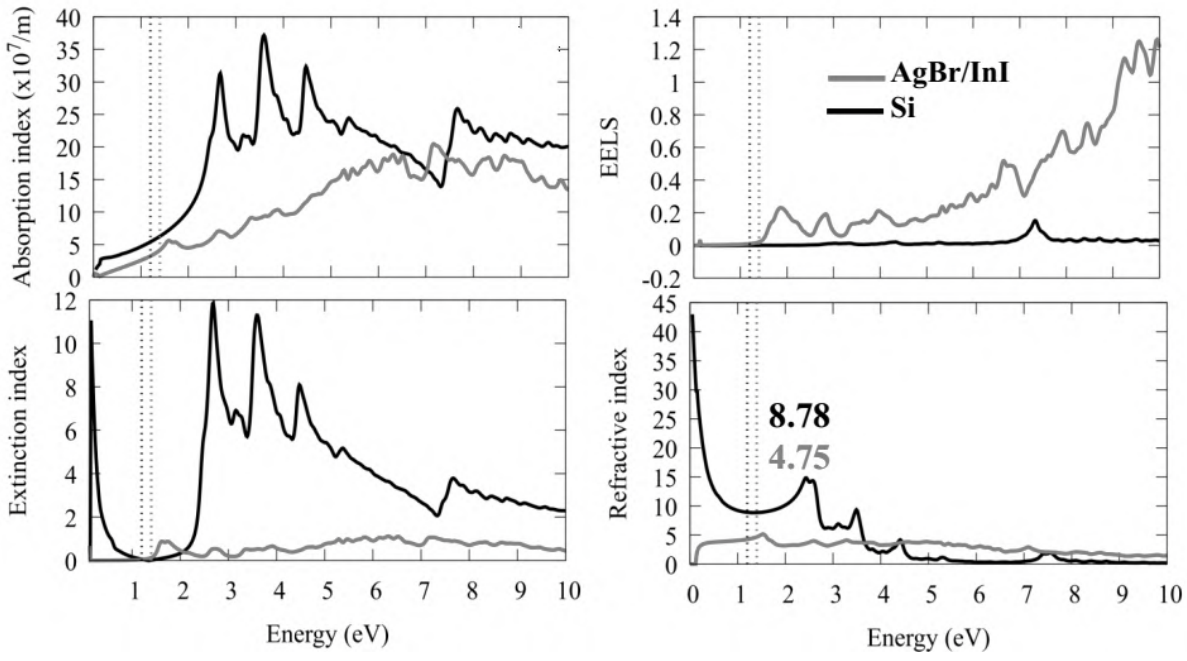

Figure 7 | Compared refractive index, absorption coefficient, extinction index and the EELS results for Si and the InI-AgBr heterostructure. The dotted black line is the *E*g point for Si and the dotted red line is the *E*g point for the InI-AgBr heterostructure.

enough for optoelectronic devices. The higher the refractive index, the higher the prospect of being able to make thin slices from the material and hence, the lesser the cost of production. All the three compounds are predicted with refractive index greater than 1, with InI-AgBr giving the best value. For optoelectronic applications, an extinction coefficient and EELS below 3 is desirable. The smaller the value the better.

According to Figure. 6, both the EELS and the extinction index are below 3 across the energy range of calculation. Silicon being a major player for fabricating electronic devices and its use still accounting for more than 80 % in energy harvesting such as in photovoltaic cell materials, it is customary to compare post-silicon efforts with silicon's performance. In this regard, the compared refractive index, absorption coefficient, extinction index, and the EELS for Si and the InI-AgBr heterostructure is given in Fig. 7. The extinction and EELS indices of InI-AgBr compares excellently well with that of Si and are < 1. The refractive index and the absorption coefficient are higher for Si than InI-AgBr heterostructure. It should be noted that the result reflected here is for single layer of the heterostructure. Stacking more layer is predicted to enhance the refractive index and the absorption coefficient far above that of Si.

4 | Conclusion

Newer semiconductors beyond silicon are needed for new and more efficient technologies. Specialized optoelectronic devices can be obtained with heterostructures due to the ability to tune them for desired property. The use of theoretical methods in this pursuit is expedient as it could help screen new chemical species to fast-track timely material discovery. The interlayer distance, bandstructure, phonon characteristics and optical indices of a new semiconductor (InI-AgBr heterostructure) relevant to optoelectronic applications have been evaluated. The bandstructure result of the individual compounds (InI and AgBr) from which the heterostructure was formed, showed a consistent trend that underscored the reliability of the results. A better optoelectronic performance was observed for the heterostructure compared with its participating constituent compounds. Stacking additional layers is predicted to enhance the various optoelectronic performance far beyond that of Si.

5 | Acknowledgement

We are grateful to the South African CHPC for granting computational resources under the MATS1181 project.

References

Baroni, S., de Gironcoli, S., Dal Corso, A., & Giannozzi, P. (2001). Phonons and related crystal properties from density-functional perturbation theory. Reviews of Modern Physics, 73(2), 515–582.

García de Arquer, F. P., Talapin, D. V., Klimov, V. I., Arakawa, Y., Bayer, M., & Sargent, E. H. (2021). Semiconductor quantum dots: Technological progress and future challenges. Science, 373(6555), eaaz8541. doi.org.

Grim, J. Q., Manna, L., & Moreels, I. (2015). A sustainable future for photonic colloidal nanocrystals. Chemical Society Reviews, 44(16), 5897-5905. DOI: 10.1039/C5CS00285K.

Giannozzi, P., Andreussi, O., Brumme, T., Bunau, O., Buongiorno Nardelli, M., Calandra, M.,Car, R., et al. (2017). Advanced capabilities for materials modelling with

Quantum ESPRESSO. Journal of Physics: Condensed Matter, 29(46), 465901-465931.

Giannozzi, P., Baseggio, O., Bonfà, P., Brunato, D., Car, R., Carnimeo, I., Cavazzoni, C., de Gironcoli, S., Delugas, P., Ferrari Ruffino, F., Ferretti, A., Marzari, N., Timrov, I., Urru, A., & Baroni, S., 2020. Quantum ESPRESSO toward the exascale. Journal of Chemical Physics, 152(15), 154105. doi: 10.1063/5.0005082.

Giannozzi, P., Baroni, S., Bonini, N., Calandra, M., Car, R., et al. (2009). Quantum ESPRESSO: A modular and open-source software project for quantum simulations of materials. Journal of Physics: Condensed Matter, 21(39), 395502.

Gjerding, M. N., Taghizadeh, A., Rasmussen, A., Ali, S., Bertoldo, F., Deilmann, T., Knøsgaard, N. R., Kruse, M., Larsen, A. H., Manti, S., Pedersen, T. G., Petralanda, U., Skovhus, T., Svendsen, M. K., Mortensen, J. J., Olsen, T., & Thygesen, K. S. (2021). Recent progress of the computational 2D materials database (C2DB). 2D materials, 8(4), Article 044002.

Khan, K. (2025). Recent developments in emerging two-dimensional materials and their applications. Molecules, 30(3), 741.

Ki, H. M., Koung, H. K., and Seung, P. P. (2025). Two-Dimensional Materials for Biosensing: Emerging Bio-Converged Strategies for Wearable and Implantable Platforms. Chemosensors, 13(6), 209.

Lin, Y. C., Torsi, R., Younas, R., & Shuck, C. E. (2023). Recent advances in 2D material theory, synthesis, properties, and applications. Nanotechnology, 34(11). https://doi.org/10.1021/acsnano.2c12759.

Lin, L., Chi, B., Wang, X., & Wilson, G. J. (2021). Inorganic electron transport materials in perovskite solar cells. Advanced Functional Materials, 31(20), 2008300.

Liu, Z. Lau, S.P. and Yan, F. (2015). Functionalized graphene and other two-dimensional materials for photovoltaic devices: device design and processing. Chemical Society Reviews 44, 5638.

Liu, Z., Qiao, Z., Li, C.-Y. and Sun, Y. (2023). Recent progress in multifunctional gas sensors based on2D materials. Chemosensors 11, 483.

Machín, A. and Márquez, F. (2024) Advancements in Photovoltaic Cell Materials: Silicon, Organic, and Perovskite Solar Cells. Materials, 17, 1165.

Merupo, V., Jose, C. Z., Alla, A., Noé, A., José, H-C., Arriaga, L.G., Ashutosh, S. and Goldie, O. (2023). *Inorganic Nanoparticles Properties and Applications*. CRC Press.

Momma, K. and Izumi, F. (2011) 'VESTA 3 for three-dimensional visualization of crystal, volumetric and morphology data' Applied Crystallography 44, 1272.

Muzibur Rahman, M., Mohammed Asiri, A., Khan, A., Inamuddin, & Tabbakh, T. (Eds). (2021). Post-Transition Metals. IntechOpen. doi: 10.5772/intechopen.90968.

Noman, M., Khan, Z and Jan, S.T. (2024). A comprehensive review on the advancements and challenges in perovskite solar cell technology. RSC Advances, 14, 5085.

Perdew, J.P., Burke, K. and Ernzerhof, M. (1996). Generalized Gradient Approximation Made Simple. Physical Review Letters, 77, 3865.

Shreya, P., Phogat, R., Jha, S., & Singh, S. (2024). Emerging advances and future prospects of two dimensional nanomaterials based solar cells. Journal of Alloys and Compounds, 1001,175063. doi:10.1016/j.jallcom.2024.175063.

Sakthivel, R., Keerthi, M., Chung, R-J. and He, J-H. (2023). Heterostructures of 2D materials

and their applications in biosensing. Prog. Mater. Sci., 132, 101024.

Shen, X., Lin, X., Peng, Y., Zhang, Y., Long, F., Han, Q., Wang, Y., & Han, L. (2024). Two-dimensional materials for highly efficient and stable perovskite solar cells. Nanomicro Letters, 16(1), 201.

Vanderbilt, D. (1990) 'Soft self-consistent pseudopotentials in a generalized eigenvalue formalism' Physical Review B 41, 7892.

Wang, Y., Li, T., Li, Y., Yang, R. and Zhang, G. (2022). 2D-materials-based wearable biosensor systems. Biosensors 12, 936.

Wu, G., Zhang, Z., Chen, J., and She, L. (2023). Ultrafast interfacial charge transfer and superior photoelectric conversion properties in one-dimensional Janus-MoSSe/WSe2 van der Waals heterostructures. Phy. Rev. B, 108, 045416.

Xuan, W., Yang, H. and Jin, G. (2023) in *Conference on Infrared, Millimeter, Terahertz Waves and Applications (IMT2022)*, Vol. 12565, 291–297.

Yuan, Z., Hou, J. and Liu, K. (2017). Interfacing 2D Semiconductors with Functional Oxides: Fundamentals, Properties, and Applications. Crystals **7**, 265.

Zhang, B., Lu, P., Tabrizian, R., Feng, P. X.-L., & Wu, Y. (2025). 2D Magnetic heterostructures: spintronics and quantum future. npj Spintronics, 2.